IEEE Access
Multidisciplinary | Rapid Review | Open Access Journal

Received June 24, 2019, accepted July 8, 2019, date of publication July 11, 2019, date of current version August 12, 2019.

Digital Object Identifier 10.1109/ACCESS.2019.2928030

Flow of a Nanofluid and Heat Transfer in Channel With Contracting/Expanding Walls

AAMIR ALI[1], YASIR ALI[1], POOM KUMAM[2,3,4], KHAN BABAR[1], ADEEL AHMED[5], AND ZAHIR SHAH[6]

[1]Department of Mathematics, COMSATS University Islamabad, Attock Campus, Attock 43600, Pakistan
[2]KMUTT-Fixed Point Research Laboratory, Room SCL 802 Fixed Point Laboratory, Science Laboratory Building, Department of Mathematics, Faculty of Science, King Mongkut's University of Technology Thonburi (KMUTT), 126 Pracha-Uthit Road, Bang Mod, Thrung Khru, Bangkok 10140, Thailand
[3]KMUTT-Fixed Point Theory and Applications Research Group, Theoretical and Computational Science Center (TaCS), Science Laboratory Building, Faculty of Science, King Mongkut's University of Technology Thonburi (KMUTT), 126 Pracha-Uthit Road, Bang Mod, Thrung Khru, Bangkok 10140, Thailand
[4]Department of Medical Research, China Medical University Hospital, China Medical University, Taichung 40402, Taiwan
[5]Department of Mathematics, COMSATS University Islamabad, Islamabad 44000, Pakistan
[6]Center of Excellence in Theoretical and Computational Science (TaCS-CoE), SCL 802 Fixed Point Laboratory, Science Laboratory Building, King Mongkut's University of Technology Thonburi (KMUTT), 126 Pracha-Uthit Road, Bang Mod, Thrung Khru, Bangkok 10140, Thailand

Corresponding author: Poom Kumam (poom.kum@kmutt.ac.th)

This work was supported by the Center of Excellence in Theoretical and Computational Science (TaCS-CoE) under the Computational and Applied Science for Smart Innovation Research Cluster (CLASSIC), Faculty of Science, KMUTT.

ABSTRACT In this paper, we have investigated the effects of nanoparticles on the flow and heat transfer of viscous fluid in a deformable porous channel. The mathematical model used for the nanofluid is Buongiorno model, which combines the Brownian diffusion and thermophoresis effects. Water is used as a base fluid. Mathematically, the problem is formulated for the flow of nanofluid generated by the expanding/contracting walls of the channel and an analytic solution using homotopy analysis method for the field quantities is presented. The numerical results are also calculated using parallel shooting method. A comparison is made of the analytic results with the numerical one to ensure the correctness of the analytic results. The effects of Brownian and thermophoresis diffusion due to nanoparticles and effect of deformation of boundaries on various physical quantities are analyzed. It is observed that the velocity is higher for expansion of the nanoparticles as compared to contraction. Also the nanoparticles increases the heat flux and decreases the mass flux. The concentration flux is higher for thermophoretic diffusion in the expanding channel.

INDEX TERMS Nanofluid, heat and mass transfer, deformable channel.

I. INTRODUCTION

The study of channel flow was first initiated by Berman [1] while studying two-dimensional steady flow of an incompressible viscous fluid between parallel porous walls. The analytic solution of this problem was presented using regular perturbation method. Subsequently, a number of studies were carried out for large and small suction/injection on the channel walls [2]–[4]. Axisymmetric flow in a deformable tube was presented by Uchida and Aoki [5] while contracting permeable wall was considered by Goto and Uchida [6]. Dauenhauer and Majdalani [7] discussed the flow between contracting/expanding parallel porous walls. A phenomenal application of the deforming channel in bio mechanics was given by Dauenhauer and Majdalani [8]. Later on Majdalani *et al.* [9] solved [8] using double perturbation technique in cross flow Reynolds number and the wall expansion ratio. Boutros *et al.* [10] presented the similarity solution of the problem using lie-group method.

In recent years, nanoscale colloidal solutions which contains fundamental condensed nano-particles are termed in the literature as Nanofluids have gained lot of intension. With the performance of a reliable model of nanofluid given by Buongiorno [11], nanofluids has become a subject of great interest for researchers and experimentalists in the last few years. We would like to refer a few papers of interest appearing in the literature; e.g, [12]–[21] and the references given there in.

Srinivas *et al.* [22] has been studied the flow of nanofluid within contracting/expanding porous pipe with chemical reaction and heat source/sink and found the analytical solution. Vijayalakshmi and Srinivas [23] has been studied the flow and heat transfer effects of a nanofluid inside expanding or contracting walls with thermal radiation. There are number

The associate editor coordinating the review of this manuscript and approving it for publication was Zhixiong Peter Li.

of applications of channels with contracting/expanding walls in industry and technology. parallel walls. Therefore, it is desirable to investigate the behavior of nanofluid for the flow generated in channels with deforming walls Its future extension for deforming tube that has a great relevance in bio-mechanics will hopefully be in easier reach. The focus of this study is thus to investigate the heat transfer effects of a nanofluid in the channel with contracting/expanding porous walls at uniform temperature. To be more precise, we intend to examine the effects of deforming boundaries on the flow in the presence of nanoparticles concentration and temperature fluxes. Mathematically, an approximate analytical solution for the velocity profile and pressure is obtained using HAM [24]–[36]. This is perhaps the best available method to find the analytical solution. Numerical results are also obtained to add credibility to the analytical results. A detailed analysis, physical aspects and important observations of this study are elaborated in section 4.

NOMENCLATURE

u, v	velocity components in $x-$ and $y-$ directions
T, C	temperature and concentration of the fluid
T_w, C_w	upper wall temperature and concentration
T_0, C_0	lower wall temperature and concentration
x, y	cartesian coordinates
t	Time
v_w	suction/injection velocity
$2a\,(t)$	channel width
D_B, D_T	Brownian diffusion and Thermophoresis diffusion coefficients
p	Pressure
A	suction/injection coefficient
k, c_p	thermal conductivity and specific heat
Pr, Sc	Prandtl and Schmidt numbers
θ, ϕ	non-dimensional temperature and concentration
Nu, Sh	Nusselt and Sherwood number
β	wall expansion ratio
ρ	Density
η	non-dimensional $y-$ coordinate
υ	kinematic viscosity
μ	fluid viscosity

II. PROBLEM FROMULATION

We consider an incompressible water based nanofluid in a two-dimensional channel of width $2a$ with x-axis along the center line and y-axis aligned vertically upward. One end of the channel is open and other end is closed with a stretchable solid membrane while the top and the bottom walls are bounded by two porous plates that allow the fluid to enter or leave during the expansion or contraction. At the upper wall the temperature and the concentration of nanoparticle fraction takes the constant values T_w and C_w respectively while at the center of channel the values are T_0 and C_o respectively. The geometry of the channel is shown in Fig.1.

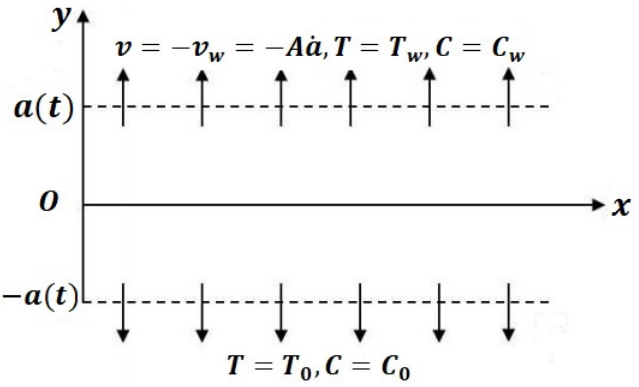

FIGURE 1. Geometry of the problem.

By using the Oberbeck–Boussinesq approximations the equations that governs the flow are [11]:

$$\frac{\partial u}{\partial x}+\frac{\partial v}{\partial y}=0, \tag{1}$$

$$\left(\frac{\partial u}{\partial t}+u\frac{\partial u}{\partial x}+v\frac{\partial u}{\partial y}\right) = \frac{-1}{\rho}\frac{\partial p}{\partial x}+\upsilon\left(\frac{\partial^2 u}{\partial x^2}+\frac{\partial^2 u}{\partial y^2}\right), \tag{2}$$

$$\left(\frac{\partial v}{\partial t}+u\frac{\partial v}{\partial x}+v\frac{\partial v}{\partial y}\right) = \frac{-1}{\rho}\frac{\partial p}{\partial y}+\upsilon\left(\frac{\partial^2 v}{\partial x^2}+\frac{\partial^2 v}{\partial y^2}\right) + g\beta_T\left(T-T_0\right), \tag{3}$$

$$\rho c_p\left(\frac{\partial T}{\partial t}+u\frac{\partial T}{\partial x}+v\frac{\partial T}{\partial y}\right) = k\left(\frac{\partial^2 T}{\partial x^2}+\frac{\partial^2 T}{\partial y^2}\right) + \rho c_p\left(D_B\left(\frac{\partial T}{\partial x}\frac{\partial C}{\partial x}+\frac{\partial T}{\partial y}\frac{\partial C}{\partial y}\right) + \frac{D_T}{T_0}\left(\left(\frac{\partial T}{\partial x}\right)^2+\left(\frac{\partial T}{\partial y}\right)^2\right)\right), \tag{4}$$

$$\frac{\partial C}{\partial t}+u\frac{\partial C}{\partial x}+v\frac{\partial C}{\partial y} = D_B\left(\frac{\partial^2 C}{\partial x^2}+\frac{\partial^2 C}{\partial y^2}\right) + D_T\left(\frac{\partial}{\partial x}\left(\frac{1}{T_0}\frac{\partial T}{\partial x}\right)+\frac{\partial}{\partial x}\left(\frac{1}{T_0}\frac{\partial T}{\partial y}\right)\right), \tag{5}$$

A two phase nanofluid model of Buongiorno [11] is adopted to incorporate the Brownian motion and thermophoresis effects [31]. The walls of the channel are contract or expand in the normal direction so that the width of the channel is a function of time. The injection/suction

velocity v_w is positive/negative according to the injection or suction which takes place due to porous walls. The appropriate boundary conditions describing the problem are:

$$\begin{aligned} u(x,a) &= 0, \quad v(x,a) = -v_w = -A\dot{a}, \\ T(x,a) &= T_w, \quad C(x,a) = C_w, \\ \frac{\partial u}{\partial y}(x,0) &= 0, \quad v(x,0) = 0, \\ T(x,0) &= T_o, \quad C(x,a) = C_o \end{aligned} \tag{6}$$

where (u, v) are the axial and normal velocity components, p is the pressure, ρ is the fluid density, k is the thermal conductivity of the material, c_p is the specific heat, D_B and D_T are the Brownian diffusion coefficient and thermophoresis diffusion coefficient and A is the injection coefficient which corresponds to the porosity of the walls. The following similarity variable and transformations will be used [9]:

$$\begin{aligned} \psi &= \frac{\upsilon x}{a(t)} F(\eta), \quad T = T_0 + (T_w - T_0)\,\theta(\eta), \\ C &= C_0 + (C_w - C_0)\,\phi(\eta), \quad \eta = \frac{y}{a(t)}, \\ u &= \frac{\upsilon x}{a^2} F'(\eta), \quad v = \frac{-\upsilon}{a} F(\eta), \\ F' &= \frac{dF}{d\eta}, \quad F = \mathrm{Re}\, f, \end{aligned} \tag{7}$$

where $\upsilon = \frac{\mu}{\rho}$ and $a(t)$ is so far arbitrary. Using Eq. (7), Eqs. (1) - (6) becomes:

$$f^{(iv)} + \beta\left(3f'' + \eta f'''\right) + \mathrm{Re}\left(ff''' - f'f''\right) - \lambda\theta' = 0, \tag{8}$$

$$\frac{1}{\mathrm{Pr}}\theta'' + \beta\eta\theta' + \mathrm{Re}\, f\theta' + N_b\theta'\phi' + N_t\left(\theta'\right)^2 = 0, \tag{9}$$

$$\frac{1}{Sc}\phi'' + \beta\eta\phi' + \mathrm{Re}\, f\phi' + \frac{1}{Sc}\frac{N_t}{N_b}\theta'' = 0. \tag{10}$$

$$\begin{aligned} f &= 0, \quad f'' = 0, \ \theta = 0, \\ \phi &= 0 \text{ at } \eta = 0 \\ f &= 1, \quad f' = 0, \ \theta = 1, \\ \phi &= 1 \text{ at } \eta = 1 \end{aligned} \tag{11}$$

where $\beta = \frac{a\dot{a}}{\upsilon}$ is the deformation parameter which is positive for expansion and negative for contraction. In order to write a self- similar equation we require

$$a = a_0\left(1 + \frac{2\upsilon\beta t}{a_0^2}\right)^{1/2}.$$

The boundary value problem is fully characterized by the following dimensionless parameters:

$$\mathrm{Re} = \frac{av_w}{\upsilon}, \quad \mathrm{Pr} = \frac{\mu c_p}{k}, \quad Sc = \frac{\mu}{\rho D},$$

TABLE 1. Comparison of the present values of velocity with numerical results and results of Majdalani *et al.* [9] and Boutros *et al.* [10].

$\beta = 0.5, Re = 5, \lambda = 0$				
η	Present Result	Numerical	[9]	[10]
0	1.55932	1.559640	1.536002	1.556324
0.05	1.55467	1.554982	1.531846	1.551780
0.10	1.54075	1.541032	1.519377	1.538164
0.15	1.51761	1.517864	1.498596	1.515522
0.20	1.48539	1.485595	1.469505	1.483935
0.25	1.44424	1.444390	1.432114	1.443517
0.30	1.39436	1.394461	1.386445	1.394421
0.35	1.33603	1.336065	1.332539	1.336839
0.40	1.26953	1.269503	1.270464	1.271006
0.45	1.19522	1.195123	1.200325	1.197207
0.50	1.11347	1.113314	1.122275	1.115778
0.55	1.02472	1.024510	1.036527	1.027110
0.60	0.929443	0.929184	0.943364	0.931656
0.65	0.828132	0.827846	0.843156	0.829933
0.70	0.721333	0.721046	0.736373	0.722523
0.75	0.60962	0.609363	0.623597	0.610078
0.80	0.493607	0.493409	0.505538	0.493322
0.85	0.373938	0.373823	0.383052	0.373046
0.90	0.251298	0.251268	0.257149	0.250109
0.95	0.126403	0.126428	0.129010	0.125435
1.0	0	0	0	0
$\beta = -0.5, Re = 5, \lambda = 0$				
η	Present Result	Numerical	[9]	[10]
0	1.49259	1.492361	1.535426	1.515104
0.05	1.48908	1.488855	1.531279	1.511345
0.10	1.47853	1.478318	1.518837	1.500051
0.15	1.46089	1.460699	1.498104	1.481177
0.20	1.43608	1.435914	1.469083	1.454653

TABLE 1. *(Continued.)* **Comparison of the present values of velocity with numerical results and results of Majdalani *et al.* [9] and Boutros *et al.* [10].**

0.25	1.40399	1.403855	1.431787	1.420383
0.30	1.36449	1.364397	1.386238	1.378261
0.35	1.31747	1.317404	1.332474	1.328174
0.40	1.26277	1.262274	1.270560	1.270018
0.45	1.20028	1.200280	1.200590	1.203708
0.50	1.12988	1.129917	1.122702	1.129200
0.55	1.05151	1.051573	1.037090	1.046507
0.60	0.965125	0.965209	0.944014	0.955722
0.65	0.870736	0.870834	0.843823	0.857047
0.70	0.768407	0.768513	0.736968	0.750818
0.75	0.658267	0.658372	0.634023	0.637541
0.80	0.540512	0.540609	0.505712	0.517928
0.85	0.415413	0.415494	0.385530	0.392938
0.90	0.283321	0.283381	0.259708	0.263822
0.95	0.144674	0.144708	0.131204	0.132178
1.0	0	0	0	0

$$Nb = \frac{\rho c_p D_B (C_w - C_0)}{\kappa}, \quad Nt = \frac{\rho c_p D_T (T_w - T_0)}{\kappa T_0},$$
$$\lambda = \frac{g\beta_T (T_w - T_0) a^4}{\upsilon^2 x},$$

where, Re, Pr, Sc, Nb, Nt and λ are the non-dimensional permeation Reynolds number (Re $>$ 0 for injection and Re $<$ 0 for suction), the Prandtl number, the Schmidt number, the Brownian diffusion parameter, the thermophoresis diffusion parameter and mixed convection parameters. The magnitude of the Brownian and the thermophoretic diffusion parameters is very small for nanoparticles [10], for example $N_b \approx 1.4 \times 10^{-10}$ and $N_t \approx 1.6 \times 10^{-7}$ for copper nanoparticles. By substituting the velocity components into Eqs. (2) and (3) we get the axial and normal pressure gradient respectively. The axial pressure is:

$$\frac{\partial p}{\partial x} = \frac{\rho \nu^2 x}{a^4}\left(F''' + \beta\left(2F' + \eta F''\right) - F'^2 + FF''\right) \quad (12)$$

Normalizing Eq. (12) by Re, we have:

$$\frac{\partial p}{\partial x} = x\left(\mathrm{Re}^{-1} f''' + \mathrm{Re}^{-1}\beta\begin{pmatrix}2f'\\+\eta f''\end{pmatrix} - f'^2 + ff''\right) \quad (13)$$

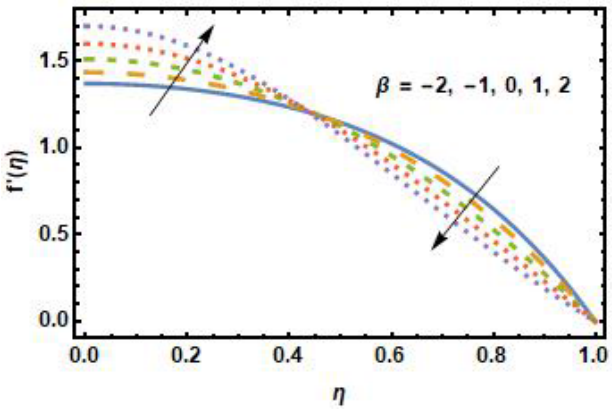

FIGURE 2. Effects of β on velocity profile when Re = 2.

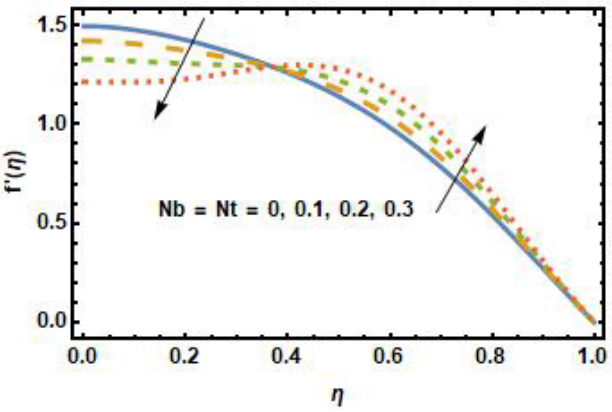

FIGURE 3. Effects of *Nb* and *Nt* velocity profile when *Re = 2* and β *= 0.5*.

The pressure distribution, for any x in the channel, can now be obtained by integrating Eq. (13), between the center line pressure p_e and the pressure at any position x.

$$\Delta p_a = \int_0^x x\begin{pmatrix}\mathrm{Re}^{-1} f'''\\+\mathrm{Re}^{-1}\beta\left(2f' + \eta f''\right) - f'^2 + ff''\end{pmatrix} \quad (14)$$

Similarly, the normal pressure gradient is:

$$\frac{\partial p}{\partial y} = -\frac{\rho \nu^2}{a^3}\left[F'' + \beta\left(F + \eta F'\right) + FF'\right] \quad (15)$$

and the normal pressure distribution is:

$$\Delta p_n = -\int_0^\eta \left(\mathrm{Re}^{-1} f'' + \mathrm{Re}^{-1}\beta\left(f + \eta f'\right) + ff'\right) \quad (16)$$

Eqs. (8) – (10) are coupled non-linear ordinary differential equations and are solved analytically by using Homotopy analysis method (HAM) [28]–[30]. To validate the analytic results, numerical solutions are also calculated using parallel shooting method and a comparison is made with the analytic results. Table 1 present the comparison of the analytical results obtained for velocity with the numerical solution and available results in the literature.

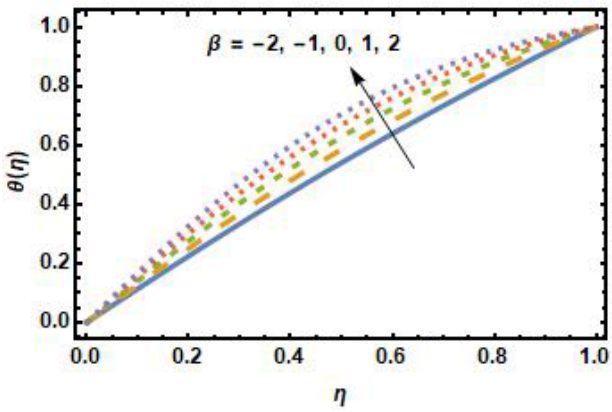

FIGURE 4. Effects of β on temperature profile.

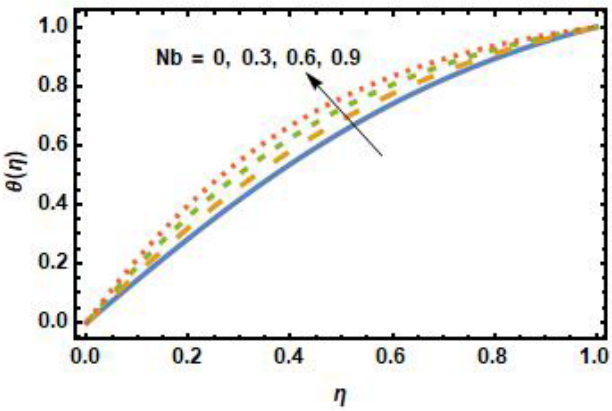

(a)

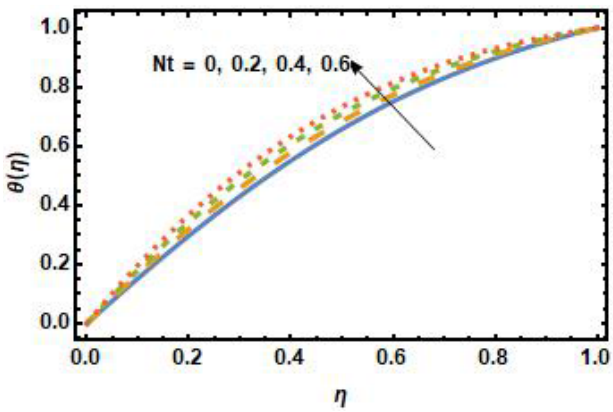

(b)

FIGURE 5. Temperature profile for various values of (a) ***Nb*** when ***Nt* = *0.1*** and (b) ***Nt*** when ***Nb* = *0.2*.**

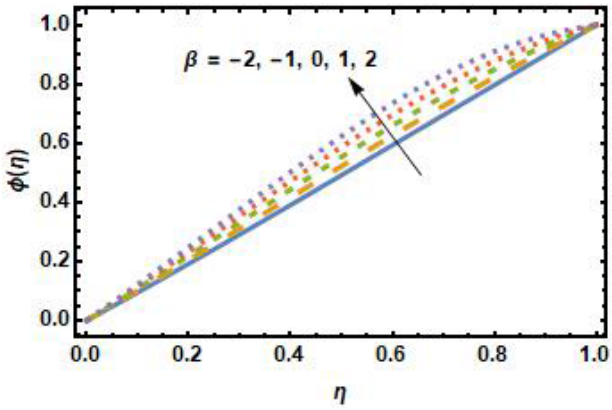

FIGURE 6. Concentration profile for various values of β.

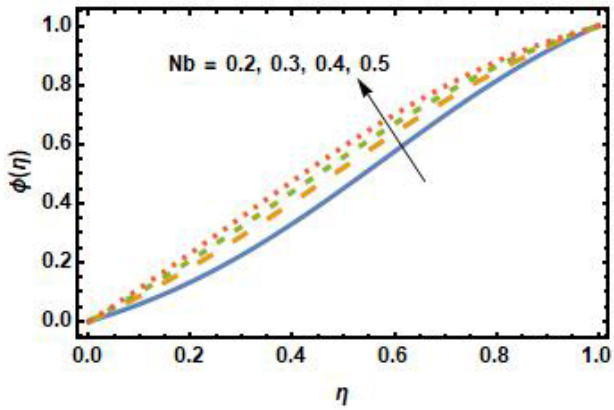

(a)

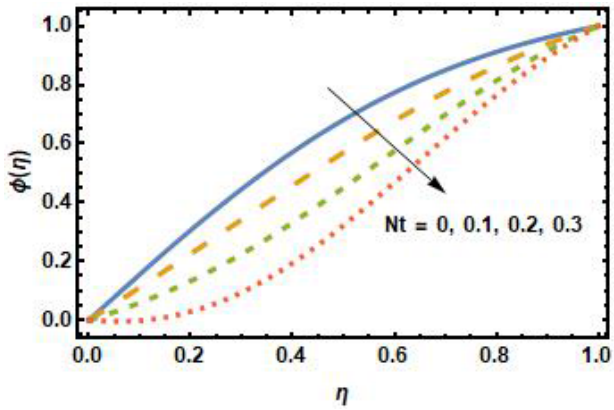

(b)

FIGURE 7. Concentration profile for various values of (a) ***Nb*** when ***Nt* = *0.2*** and (b) ***Nt*** when ***Nb* = *0.2*.**

III. RESULTS AND DISCUSSION

We propose nanofluid in deforming channels and analyze the effects of Nb, Nt and the deformation parameter β on the flow generated by deforming channel. To begin with, we observe the effects of deformation parameter β on the velocity profile in Fig. 2. The velocity near the boundary $\eta = 1$ decreases for increasing value of β while it increases in the center of the channel which confirming that the inertia is controlled by the deformation of the channel. The rate at which the velocity is changes is higher when the channel is expanding ($\beta > 0$) as compared to when it is contracting ($\beta < 0$). The combined effects of Brownian diffusion and thermophoresis diffusion parameters on the velocity profile are presented in Fig. 3. It is observed that the velocity is increasing near the wall while it is decreasing in the center of the channel when we increase the values of Brownian diffusion and thermophoresis diffusion parameters.

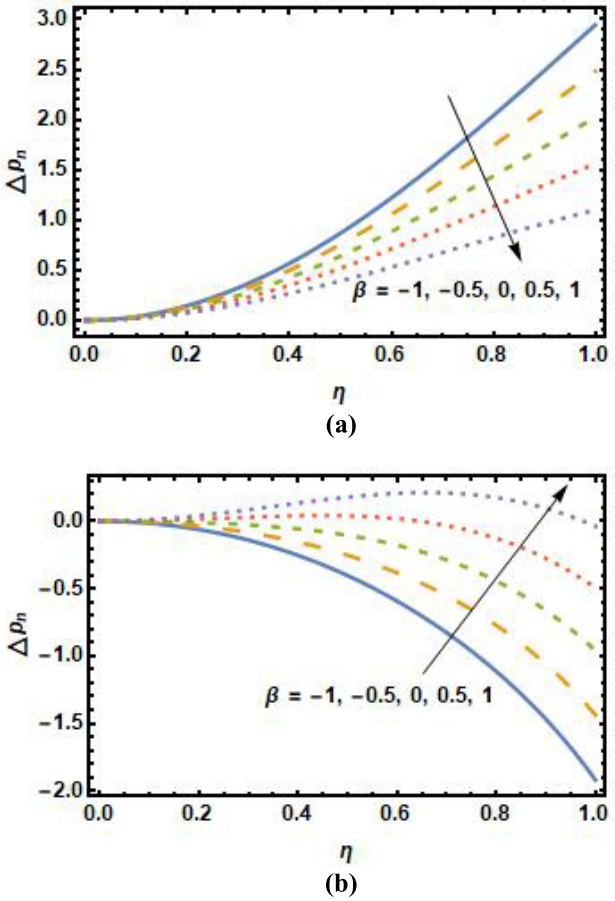

FIGURE 8. Normal pressure gradient for various values of β (a) when Re = 1.0 and (b) when Re = −1.0.

Dependence of temperature on the deformation is shown in Fig. 4 taking the values $\mathrm{Re} = 2.0, \mathrm{Pr} = 0.7, Sc = 0.6$, $Nt = Nb = 0.2$ and $\lambda = 2$. It is observed that the temperature across the channel increases for expanding channel and decreases for contracting channel. The temperature of the fluid is increased or decreased with the gap between the heated walls is increased for expanding and decreased for contracting channel.

In Fig. 5 the effects of nanoparticles on the temperature distribution is examined by taking $\beta = 0.5, \mathrm{Re} = 1, \mathrm{Pr} = 1.2$, $Sc = 1$ and $\lambda = 2$. The temperature of the fluid will increase by increasing the magnitude of the Brownian diffusion parameter. This effect can be seen from Fig. 5 (a) in which the curve with lower temperature corresponds to lowest value of Brownian diffusion parameter. The effects of Nt on the temperature of the nanofluid are shown in Fig. 5 (b). It is observed that an increase in the values of Nt increases the temperature of the fluid because Nt increases the thermal diffusivity of the nanoparticles that accelerates the temperature of the nanofluid.

Fig. 6 shows the concentration profile for various values of deformation parameter fixing $\mathrm{Re} = 2.0, \mathrm{Pr} = 1.2, Sc = 1$, $Nt = 0.1, Nb = 0.2$ and $\lambda = 1$. Further the concentration of nanoparticles is observed to be higher within the channel while it is expanding i.e. β increasing from zero to positive values whereas concentration reduces for contraction.

In Fig. 7 the behavior of nanoparticles concentration for varying Brownian and thermophoresis diffusion parameters is shown. Increase in Brownian diffusion parameter Nb refers to increase in number of nanoparticles causing an increase Brownian diffusion. Thus higher concentration of nanoparticles corresponds to higher Nb which can also be seen from Fig. 7 (a). Fig. 7 (b) describes the effect of thermophoresis diffusion on nanoparticles concentration. It is observed that a higher concentration profile correspond to lower thermophoresis diffusion.

In Fig. 8 we show the normal pressure gradient for various values of deformation parameter β for (a) injection and for (b) suction. For the case of injection the pressure gradient decreases with increasing β while it increases for the case of suction, i.e. the normal pressure gradient drops for positive values and rises for negative values of Re independent of β.

TABLE 2. Numerical Values of Skin Friction Coefficient for Different Re, β, Nb and Nt.

Re	β	Nb	$N\tau$	$-f''(1)$
-2.0	0.5	0.2	0.1	2.07691
-1.0				2.20613
0				2.33674
1.0				2.56144
2.0				2.67339
1.0	-1.0	0.2	0.1	3.39558
	-0.5			3.09842
	0			2.82301
	0.5			2.56144
	1.0			2.30586
1.0	0.5	0	0.1	2.48351
		0.2		2.56144
		0.4		2.64259
		0.6		2.72494
		0.8		2.8065
1.0	0.5	0.2	0	2.51934
			0.1	2.56144
			0.2	2.60398
			0.3	2.64634
			0.4	2.68789

Table 2 shows the numerical values of heat transfer for various values of Reynolds number Re, deformation parameter β, Brownian diffusion parameter Nb and thermophoresis diffusion parameter Nt. It is observed that the value of skin friction coefficient decreases for increasing values of the deformation parameter, the Brownian diffusion and thermophoresis diffusion parameters while it is increasing for increasing Reynolds number.

In Fig. 9 Nusselt number Nu is plotted for varying Brownian diffusion and thermophoretic diffusion parameters against

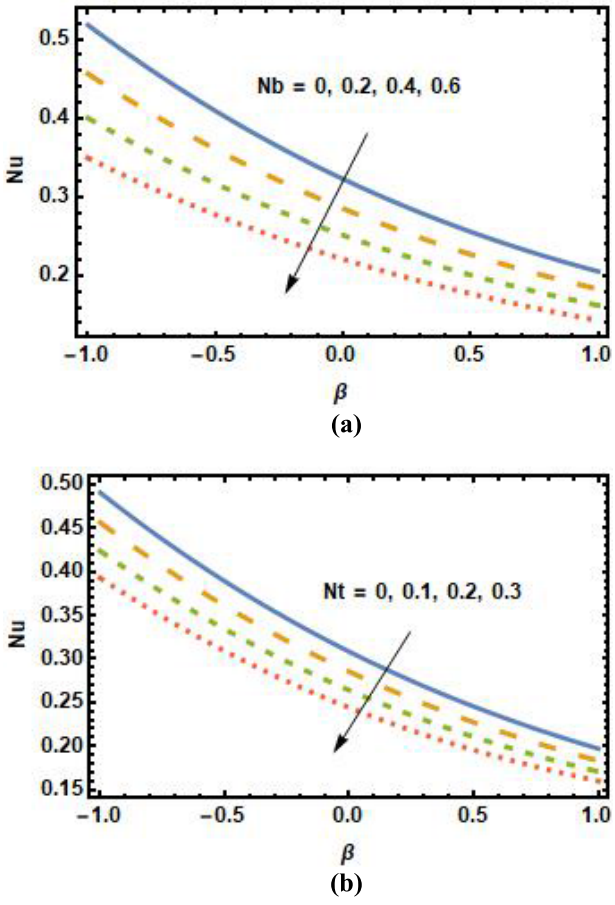

FIGURE 9. Nusselt number against β for (a) *Nb* (b) *Nt*.

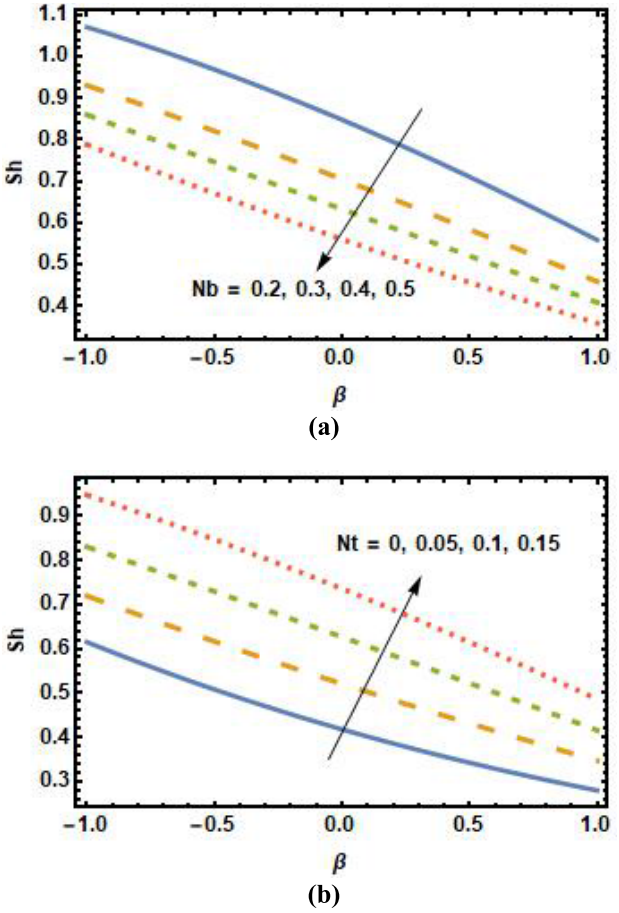

FIGURE 10. Sherwod number against β for (a) *Nb* (b) *Nt*.

deformation parameters showing the behavior of heat flux at the upper plate. It is observed that heat flux at the surface is a decreasing function of nanoparticle properties. In other words, heat flux at the surface decreases in the presence of nanoparticles and can be controlled by varying the quantity and quality of nanoparticles. It is obvious from Fig. 5 (a) and (b) that the temperature is increasing function of nanoparticles so heat flux must be a decreasing function. The most interesting observation comes through the effects of nanoparticles on Nusselt number for deforming channel. Nusselt number is independent of the deformation of boundaries i.e. *Nu* is an increasing function of *Nb* and *Nt* for contracting ($\beta < 0$), expanding ($\beta > 0$) as well as fixed wall ($\beta = 0$) channels.

In Fig. 10, Sherwood number *Sh* i.e. nanoparticles concentration flux at the upper plate of the channel is plotted for varying Brownian diffusion and thermophoretic diffusion parameters against deformation parameter. It is observed Sherwood number is a decreasing function of Brownian diffusion parameter while it is an increasing function of thermophoretic diffusion parameter for all values of β. The reason for this behavior can be verified from Fig. 7 (a) and (b). A worth mentioning observation is that the rate of change of Sherwood number with respect to thermophoretic diffusion parameter *Nt* is higher for expanding channel as compared to contracting channel.

IV. CONCLUSION

In this study, we have investigated the heat and mass transfer analysis of a Nanofluid inside parallel walls which are deforming. The effects of nanoparticles and contraction/expansion of channel walls on the flow of nanofluid is investigated through analytical considerations. The important observations are:

1. The velocity is higher at the center for expanding channel as compared to contracting.
2. Presence of nanoparticles enhances the heat flux at the surface and can be controlled by varying the quantity and quality of nanoparticles.
3. Concentration flux decreases for increasing thermophoretic diffusion parameter and increases for Brownian diffusion parameter.
4. Heat transfer rate at the surface increases for increasing thermophoretic diffusion parameter is higher for expanding channel as compared to contracting channel.
5. mass transfer rate at the surface increases for increasing Brownian diffusion parameter is higher for expanding channel as compared to contracting channel.

APPENDIX
HOMOTOPY ANALYSIS METHOD (HAM)

The initial guesses and auxiliary linear operators for the dimensionless Eqs. (8) – (10) subject to boundary conditions (11) are denoted by f_0, θ_0, ϕ_0, and L_f, L_θ, L_ϕ and are defined as:

$$f_0(\eta) = \frac{1}{2}\eta\left(3-\eta^2\right)$$
$$\theta_0(\eta) = \phi_0(\eta) = \eta \tag{A1}$$

and

$$L_f = \frac{d^4 f}{d\eta^4}, \quad L_\theta = \frac{d^2\theta}{d\eta^2}, \quad L_\phi = \frac{d^2\phi}{d\eta^2}. \tag{A2}$$

with

$$L_f\left[c_1 + c_2\eta + c_3\eta^2 + c_4\eta^3\right] = 0,$$
$$L_\theta\left[c_5 + c_6\eta\right] = 0,$$
$$L_\phi\left[c_7 + c_8\eta\right] = 0 \tag{A3}$$

where c_i, $(i = 1-8)$ are the arbitrary constants. The zeroth and m^{th} – order deformation problems are:

A. ZEROTH-ORDER PROBLEM

$$\begin{aligned}
&(1-p)\,L_f\left[f(\eta,p) - f_0(\eta)\right] \\
&\quad = p\hbar_f \Im_f\left[f(\eta,p),\ \theta(\eta,p),\ \phi(\eta,p)\right], \\
&(1-p)\,L_\theta\left[\theta(\eta,p) - \theta_0(\eta)\right] \\
&\quad = p\hbar_\theta \Im_\theta\left[f(\eta,p),\ \theta(\eta,p),\ \phi(\eta,p)\right], \\
&(1-p)\,L_\phi\left[\phi(\eta,p) - \phi_0(\eta)\right] \\
&\quad = p\hbar_\phi \Im_\phi\left[f(\eta,p),\ \theta(\eta,p),\ \phi(\eta,p)\right],
\end{aligned} \tag{A4}$$

with

$$\begin{aligned}
&f(0,p) = 0, \quad f''(0,p) = 0, \quad f(1,p) = 1, \\
&f'(1,p) = 0, \quad \theta(0,p) = 0, \quad \theta(1,p) = 0, \\
&\phi(0,p) = 0, \quad \phi(1,p) = 0,
\end{aligned} \tag{A5}$$

and

$$\begin{aligned}
&\Im_f\left[f(\eta,p), \theta(\eta,p), \phi(\eta,p)\right] \\
&= \frac{\partial^4 f(\eta,p)}{\partial\eta^4} \\
&\quad + \beta\left(3\frac{\partial^2 f(\eta,p)}{\partial\eta^2} + \eta\frac{\partial^3 f(\eta,p)}{\partial\eta^3}\right) \\
&\quad + \mathrm{Re}\left(f(\eta,p)\frac{\partial^3 f(\eta,p)}{\partial\eta^3} - \frac{\partial f(\eta,p)}{\partial\eta}\right. \\
&\quad \left.\times \frac{\partial^2 f(\eta,p)}{\partial\eta^2}\right),
\end{aligned} \tag{A6}$$

$$\begin{aligned}
&\Im_\theta\left[f(\eta,p), \theta(\eta,p), \phi(\eta,p)\right] \\
&= \frac{\partial^2\theta(\eta,p)}{\partial\eta^2} + \mathrm{Pr}\,\eta\frac{\partial\theta(\eta,p)}{\partial\eta} \\
&\quad + \mathrm{Pr}\,\mathrm{Re}\, f(\eta,p)\frac{\partial\theta(\eta,p)}{\partial\eta} \\
&\quad + \mathrm{Pr}\,\mathrm{Nb}\frac{\partial\theta(\eta,p)}{\partial\eta}\frac{\partial\phi(\eta,p)}{\partial\eta} \\
&\quad + \mathrm{Pr}\,Nt\left(\frac{\partial\theta(\eta,p)}{\partial\eta}\right)^2,
\end{aligned} \tag{A7}$$

$$\begin{aligned}
&\Im_\phi\left[f(\eta,p),\ \theta(\eta,p),\ \phi(\eta,p)\right] \\
&= \frac{\partial^2\phi(\eta,p)}{\partial\eta^2} + Sc\eta\frac{\partial\phi(\eta,p)}{\partial\eta} \\
&\quad + Sc\,\mathrm{Re}\, f(\eta,p)\frac{\partial\phi(\eta,p)}{\partial\eta} \\
&\quad + \frac{Nt}{Nb}\frac{\partial^2\theta(\eta,p)}{\partial\eta^2},
\end{aligned} \tag{A8}$$

where $p \in [0,1]$ represents the embedding parameter and $\hbar_f, \hbar_\theta$ and $\hbar_\phi$ are the non-zero auxiliary parameters.

B. m^{th}-ORDER PROBLEM

$$\begin{aligned}
L_f\left[f_m(\eta) - \chi f_{m-1}(\eta)\right] &= \hbar_f \Im_m^f(\eta), \\
L_\theta\left[\theta_m(\eta) - \chi\theta_{m-1}(\eta)\right] &= \hbar_\theta \Im_m^\theta(\eta), \\
L_\phi\left[\phi_m(\eta) - \chi\phi_{m-1}(\eta)\right] &= \hbar_\phi \Im_m^\phi(\eta),
\end{aligned} \tag{A9}$$

with

$$\begin{aligned}
&f_m(0) = 0, \quad f_m''(0) = 0, \\
&f_m(1) = 0, \quad f_m'(1) = 0, \\
&\theta_m(0) = 0, \quad \theta_m(1) = 0, \\
&\phi_m(0) = 0, \quad \phi_m(1) = 0,
\end{aligned} \tag{A10}$$

and

$$\begin{aligned}
\Im_m^f(\eta) &= f_{m-1}^{(iv)} + \beta\sum_{k=0}^{m-1}\left(3f_{m-1}'' + \eta f_{m-1}'''\right) \\
&\quad + \mathrm{Re}\sum_{k=0}^{m-1}\sum_{l=0}^{k}\left(f_{m-l-k}f_k''' - f_{m-l-k}'f_k''\right),
\end{aligned} \tag{A11}$$

$$\begin{aligned}
\Im_m^\theta(\eta) &= \theta_{m-1}'' + \mathrm{Pr}\,\eta\sum_{k=0}^{m-1}\theta_{m-1}' \\
&\quad + \mathrm{Pr}\sum_{k=0}^{m-1}\sum_{l=0}^{k}\left(Ref_{m-l-k}\theta_k' + Nb\theta_{m-l-k}'\phi_k'\right. \\
&\quad \left. + Nt\theta_{m-l-k}'\theta_k'\right),
\end{aligned} \tag{A12}$$

$$\begin{aligned}
\Im_m^\phi(\eta) &= \phi_{m-1}'' + Sc\eta\sum_{k=0}^{m-1}\phi_{m-1}' \\
&\quad + Sc\sum_{k=0}^{m-1}\sum_{l=0}^{k}\left(\mathrm{Re}\, f_{m-l-k}\phi_k' + \frac{Nt}{Nb}\theta_{m-l-k}''\theta_k''\right),
\end{aligned} \tag{A13}$$

for $p = 0$ and $p = 1$, we can write

$$\begin{aligned} f(\eta, 0) &= f_0(\eta), \quad f(\eta, 1) = f(\eta), \\ \theta(\eta, 0) &= \theta_0(\eta), \quad \theta(\eta, 1) = \theta(\eta), \\ \phi(\eta, 0) &= \phi_0(\eta), \quad \phi(\eta, 1) = \phi(\eta), \end{aligned} \tag{A14}$$

where p varies from 0 to 1, $f(\eta, p)$, $\theta(\eta, p)$ and $\phi(\eta, p)$ varies from the initial solution $f_0(\eta)$, $\theta_0(\eta)$ and $\phi_0(\eta)$ to the final solutions $f(\eta)$, $\theta(\eta)$ and $\phi(\eta)$. By Taylor's series we have:

$$\begin{aligned} f(\eta, p) &= f_0(\eta) + \sum_{m=1}^{\infty} f_m(\eta) p^m, \quad f_m(\eta) \\ &= \frac{1}{m!} \left. \frac{\partial^m f(\eta, p)}{\partial p^m} \right|_{p=0}, \\ \theta(\eta, p) &= \theta_0(\eta) + \sum_{m=1}^{\infty} \theta_m(\eta) p^m, \quad \theta_m(\eta) \\ &= \frac{1}{m!} \left. \frac{\partial^m \theta(\eta, p)}{\partial p^m} \right|_{p=0}, \\ \phi(\eta, p) &= \phi_0(\eta) + \sum_{m=1}^{\infty} \phi_m(\eta) p^m, \quad \phi_m(\eta) \\ &= \frac{1}{m!} \left. \frac{\partial^m \phi(\eta, p)}{\partial p^m} \right|_{p=0}, \end{aligned} \tag{A15}$$

the values of auxiliary parameter is chosen in such a way that the series (A15) converge at $p = 1$, i.e.

$$\begin{aligned} f(\eta) &= f_0(\eta) + \sum_{m=1}^{\infty} f_m(\eta), \\ \theta(\eta) &= \theta_0(\eta) + \sum_{m=1}^{\infty} \theta_m(\eta), \\ \phi(\eta) &= \phi_0(\eta) + \sum_{m=1}^{\infty} \phi_m(\eta). \end{aligned} \tag{A16}$$

The general solutions f_m, θ_m and ϕ_m of Eqs. (8) – (10) in terms of special solutions f_m^*, θ_m^* and ϕ_m^* and are given by:

$$\begin{aligned} f_m(\eta) &= f_m^*(\eta) + c_1 + c_2\eta + c_3\eta^2 + c_4\eta^3, \\ \theta_m(\eta) &= \theta_m^*(\eta) + c_5 + c_6\eta, \\ \phi_m(\eta) &= \phi_m^*(\eta) + c_7 + c_8\eta, \end{aligned} \tag{A17}$$

where the constants c_i $(i = 1 - 8)$ through the boundary conditions (11).

CONFLICTS OF INTEREST

The author declares that they have no competing interests.

ACKNOWLEDGMENT

This project was supported by the Theoretical and Computational Science (TaCS) Center under Computational and Applied Science for Smart Innovation Research Cluster (CLASSIC), Faculty of Science, KMUTT.

REFERENCES

[1] A. S. Berman, "Laminar flow in channels with porous walls," *J. Appl. Phys.*, vol. 24, no. 9, pp. 1232–1235, Dec. 1953.
[2] J. R. Sellars, "Laminar flow in channels with porous walls at high suction Reynolds numbers," *J. Appl. Phys.*, vol. 26, no. 4, pp. 489–490, 1955.
[3] G. Taylor, "Fluid flow in regions bounded by porous surfaces," *Proc. Roy. Soc. London. A, Math. Phys. Sci.*, vol. 234, no. 1199, pp. 456–475, Mar. 1956.
[4] R. M. Terrill, "Laminar flow in a uniformly porous channel with large injection," *Aeronautical Quart.*, vol. 15, no. 3, p. 323, Aug. 1964.
[5] S. Uchida and H. Aoki, "Unsteady flows in a semi-infinite contracting or expanding pipe," *J. Fluid Mech.*, vol. 82, no. 2, pp. 371–387, Sep. 1977.
[6] M. Goto and S. Uchida, "Unsteady flows in a semi-infinite contracting or expanding pipe with injection through wall," *Trans. Jpn. Soc. Aeronautical Space Sci.*, vol. 33, pp. 14–27, 1990.
[7] E. C. Dauenhauer and J. Majdalani, "Unsteady flows in semi-infinite expanding channels with wall injection," in *Proc. AIAA*, 1999, pp. 3523–3599.
[8] E. C. Dauenhauer and J. Majdalani, "Exact self-similarity solution of the Navier-Stokes equations for a deformable channel with wall suction or injection," in *Proc. AIAA*, 2001, pp. 2001–3588.
[9] J. Majdalani, C. Zhou, and C. A. Dawson, "Two-dimensional viscous flow between slowly expanding or contracting walls with weak permeability," *J. Biomech.*, vol. 35, no. 10, pp. 1399–1403, Oct. 2002.
[10] Y. Z. Boutros, M. B. Abd-el-Malek, N. A. Badran, and H. S. Hassan, "Lie-group method solution for two-dimensional viscous flow between slowly expanding or contracting walls with weak permeability," *Appl. Math. Model.*, vol. 31, no. 6, pp. 1092–1108, Jun. 2007.
[11] J. Buongiorno, "Convective transport in nanofluids," *J. Heat Transf.*, vol. 128, no. 3, pp. 240–250, Aug. 2006.
[12] M. Turkyilmazoglu, "Nanofluid flow and heat transfer due to a rotating disk," *Comput. Fluids*, vol. 94, pp. 139–146, May 2014.
[13] A. Ahmad, S. Asghar, and A. Alsaedi, "Flow and heat transfer of a nanofluid over a hyperbolically stretching sheet," *Chin. Phys. B*, vol. 23, no. 7, 2014, Art. no. 074401.
[14] S. Nadeem, R. Ul Haq, and Z. N. Khan, "Numerical solution of non-newtonian nanofluid flow over a stretching sheet," *Appl. Nanosci.*, vol. 4, no. 5, pp. 625–631, Jun. 2014.
[15] T. Hayat, F. M. Abbasi, M. Al-Yami, and S. Monaquel, "Slip and Joule heating effects in mixed convection peristaltic transport of nanofluid with Soret and Dufour effects," *J. Mol. Liquids*, vol. 194, pp. 93–99, Jun. 2014.
[16] A. Ahmad, S. Asghar, and S. Afzal, "Flow of nanofluid past a Riga plate," *J. Magn. Magn. Mater.*, vol. 402, pp. 44–48, Mar. 2016.
[17] T. Hayat, I. Ullah, A. Alsaedi, and M. Farooq, "MHD flow of Powell-Eyring nanofluid over a non-linear stretching sheet with variable thickness," *Results Phys.*, vol. 7, pp. 189–196, Jan. 2017.
[18] K. Hosseinzadeh, A. J. Amiri, S. S. Ardahaie, and D. D. Ganji, "Effect of variable lorentz forces on nanofluid flow in movable parallel plates utilizing analytical method," *Case Stud. Therm. Eng.*, vol. 10, pp. 595–610, Sep. 2017.
[19] S. S. Ghadikolaei, K. Hosseinzadeh, D. D. Ganji, and B. Jafari, "Nonlinear thermal radiation effect on magneto Casson nanofluid flow with Joule heating effect over an inclined porous stretching sheet," *Case Stud. Therm. Eng.*, vol. 12, pp. 176–187, Sep. 2018.
[20] M. Gholinia, S. Gholinia, H. Kh, and D. D. Ganji, "Investigation on ethylene glycol nano fluid flow over a vertical permeable circular cylinder under effect of magnetic field," *Results Phys.*, vol. 9, pp. 1525–1533, Jun. 2018.
[21] A. Ali, A. Sajjad, and S. Asghar, "Thermal-diffusion and diffusion-thermo effects in a nanofluid flow with non-uniform heat flux and convective walls," *J. Nanofluids*, vol. 8, no. 6, pp. 1367–1375, Jun. 2019.
[22] S. Srinivas, A. Vijayalakshmi, A. S. Reddy, and T. R. Ramamohan, "MHD flow of a nanofluid in an expanding or contracting porous pipe with chemical reaction and heat source/sink," *Propuls. Power Res.*, vol. 5, no. 2, pp. 134–148, Jun. 2016.
[23] V. Akula and S. Srinivas, "Asymmetric flow of a nanofluid between expanding or contracting permeable walls with thermal radiation," *Frontiers Heat Mass Transf.*, vol. 7, no. 1, pp. 1–11, May 2016.
[24] S. Liao, *Beyond Perturbation: Introduction to Homotopy Analysis Method*. Boca Raton, FL, USA: CRC Press, 2003.
[25] S. Abbasbandy, "The application of homotopy analysis method to non-linear equations arising in heat transfer," *Phys. Lett. A*, vol. 360, no. 1, pp. 109–113, Dec. 2006.

[26] S. Abbasbandy, "Homotopy analysis method for heat radiation equations," *Int. Commun. Heat Mass Transf.*, vol. 34, no. 3, pp. 380–387, Mar. 2007.
[27] S. Abbasbandy, "Approximate solution for the nonlinear model of diffusion and reaction in porous catalysts by means of the homotopy analysis method," *Chem. Eng. J.*, vol. 136, nos. 2–3, pp. 144–150, Mar. 2008.
[28] M. M. Rashidi, G. Domairry, and S. Dinarvand, "Approximate solutions for the Burger and regularized long wave equations by means of the homotopy analysis method," *Commun. Nonlinear Sci. Numer. Simul.*, vol. 14, no. 3, pp. 708–717, Mar. 2009.
[29] S. Nadeem and S. Salman, "Analytical treatment of unsteady mixed convection MHD flow on a rotating cone in a rotating frame," *J. Taiwan Inst. Chem. Eng.*, vol. 44, no. 4, pp. 596–604, Jul. 2013.
[30] T. Hayat, A. Aziz, T. Muhammad, and B. Ahmad, "On magnetohydrodynamic flow of second grade nanofluid over a nonlinear stretching sheet," *J. Magn. Magn. Mater.*, vol. 408, pp. 99–106, Jun. 2016.
[31] T. Hayat, R. Sajjad, A. Alsaedi, T. Muhammad, and R. Ellahi, "On squeezed flow of couple stress nanofluid between two parallel plates," *Results Phys.*, vol. 7, pp. 553–561, Jan. 2017.
[32] M. Turkyilmazoglu, "Buongiorno model in a nanofluid filled asymmetric channel fulfilling zero net particle flux at the walls," *Int. J. Heat Mass Transf.*, vol. 126, Nov. 2018, pp. 974–979.
[33] N. S. Khan, T. Gul, S. Islam, and W. Khan, "Thermophoresis and thermal radiation with heat and mass transfer in a magnetohydrodynamic thin-film second-grade fluid of variable properties past a stretching sheet," *Eur. Phys. J. Plus*, vol. 132, p. 11, Jan. 2017.
[34] W. Khan, M. Idrees, T. Gul, K. M. Altaf, and E. Bonyah, "Three non-newtonian fluids flow considering thin film over an unsteady stretching surface with variable fluid properties," *Adv. Mech. Eng.*, vol. 10, no. 10, Oct. 2018, Art. no. 1687814018807361.
[35] T. Gul, "Scattering of a thin layer over a nonlinear radially extending surface with magneto hydrodynamic and thermal dissipation," *Surf. Rev. Lett.*, vol. 26, no. 1, Jan. 2019, Art. no. 1850123.
[36] A. Shojaei, A. J. Amiri, S. S. Ardahaie, K. Hosseinzadeh, and D. D. Ganji, "Hydrothermal analysis of non-newtonian second grade fluid flow on radiative stretching cylinder with Soret and Dufour effects," *Case Stud. Therm. Eng.*, vol. 13, Mar. 2019, Art. no. 100384.

AAMIR ALI received the Master of Science and Ph.D. degrees in mathematics from COMSATS University Islamabad, Attock Campus, where he is currently an Assistant Professor with the Department of Mathematics. He has published several research articles in international journals. His areas of research interests include Newtonian and non-Newtonian fluids flow, nanofluid, heat transfer analysis, magnetohydrodynamics, channel flow, and analytical solutions.

YASIR ALI is currently pursuing the Master of Science degree in mathematics from COMSATS University Islamabad, Attock Campus.

POOM KUMAM received the Ph.D. degree in mathematics from Naresuan University, Thailand. He is currently a Full Professor with the Department of Mathematics, King Mongkut's University of Technology Thonburi (KMUTT). He is also the Head of the Theoretical and Computational Science Center (TaCS-Center) and the KMUTT Fixed Point Theory and Applications Research Group, KMUTT. In addition, he is the Director of Computational and Applied Science for Smart Innovation Cluster (CLASSIC Research Cluster), KMUTT. He has authored or coauthored more than 400 international peer-reviewed journals and his main research interests include fixed point theory and applications and computational fixed point algorithms.

KHAN BABAR is currently pursuing the Master of Science degree in mathematics from COMSATS University Islamabad, Attock Campus.

ADEEL AHMED received the B.S., M.S. and Ph.D. degrees in mathematics from COMSATS University Islamabad, where he is currently an Assistant Professor with the Department of Mathematics. He has published several papers in various topics of fluid mechanics. His research interests include simulations, Newtonian and non-Newtonian fluids, heat transfer analysis, nonlinear science, and magnetohydrodynamic.

ZAHIR SHAH received the M.Sc. degree from the University of Malaknad lower Dir chakdara, KPK, Pakistan, the M.Phil. degree from the Islamia College University Peshawar Pakistan, and the Ph.D. degree from Abdul Wali Khan University Mardan, Pakistan. He is currently a Postdoctoral with the SCL 802 Fixed Point Laboratory, Science Laboratory Building, Center of Excellence in Theoretical and Computational Science (TaCS-CoE), King Mongkut's University of Technology Thonburi (KMUTT), Bangkok, Thailand. His research interests include nanofluid, CFD, simulation, heat transfer, MHD, hall effect, mesoscopic modeling, nonlinear science, magnetohydrodynamic, ferrohydrodynamic, electrohydrodynamic, and heat exchangers.